Experimental investigation of rubidium atoms above the field-ionization limit using a time-resolved wave packet approach

Broers, B.; Christian, J.F.; van Linden van den Heuvell, H.B.

DOI
10.1103/PhysRevA.49.2498

Publication date
1994

Published in
Physical Review A

Experimental investigation of rubidium atoms above the field-ionization limit using a time-resolved wave packet approach

B. Broers,[1] J. F. Christian,[1] and H. B. van Linden van den Heuvell[1,2]
[1] *Fundamenteel Onderzoek der Materie—Instituut voor Atoom-en Molecuulfysica, Kruislaan 407, 1098 SJ Amsterdam, The Netherlands*
[2] *Van der Waals-Zeeman Laboratory, Valckenierstraat 65, 1018 XE Amsterdam, The Netherlands*
(Received 30 August 1993)

We have performed a time-resolved study of the behavior of Rb atoms in electric fields (0.1–3 kV/cm) at energies close to and above the field-ionization threshold. This is done using a pair of picosecond laser pulses that creates an electronic wave packet and monitors its evolution in terms of the time-autocorrelation function. In the discussion of the results, emphasis is put on the relation with the classical picture of field ionization, *viz.* the escape of an electron over the saddle point in the potential energy. This picture is found to be capable of qualitatively explaining the observed dependences on excitation energy and light polarization. Furthermore, the observed dynamics as a function of field strength is shown to be in agreement with the general scaling properties of the Hamiltonian of hydrogen, which also accounts for the measured time periods quantitatively. The relation between time- and frequency-domain measurements is shortly addressed, as is the question of why a hydrogenic approximation explains the observed dominant features adequately.

PACS number(s): 32.60.+i, 32.80.Rm, 32.80.Fb

I. INTRODUCTION

The properties of highly excited states (Rydberg states) in atoms have been given considerable attention over the last decades, especially after the advent of wavelength-tunable laser systems which made these states experimentally accessible [1,2]. Many investigations concentrated on their behavior in external electric and magnetic fields, particularly in the regime where these fields have strengths comparable to the Coulomb field of the atomic core. For magnetic fields, much work has been inspired by the measurements of Garton and Tomkins [3], who observed a modulation in the photoabsorption spectrum of barium around the ionization limit. In the case of electric fields, the extensive studies by the group of Kleppner [4], which included panoramic Stark maps above the classical field ionization threshold [5], have been important. Also the pioneering experiment by Freeman *et al.*, [6] in which the first observation of a modulated photoabsorption spectrum above the zero-field ionization threshold was reported, has received a lot of attention.

In most experimental studies, including those mentioned above, the photoabsorption spectrum was measured by scanning the frequency of a laser. This method, in combination with a level-by-level analysis, may not always be the one that provides the most insight into the physics of the system, because of the infinite number of densely packed levels near the ionization limit. It is therefore desirable to bring out only a limited number of parameters that still characterize the system well. A rather powerful method which fulfills this requirement is scaled-energy spectroscopy, in which the excitation frequency is scanned while at the same time the strength of the external field is changed according to the scaling properties of the classical Hamiltonian. Even though the spectra recorded in this way may seem completely irregular, their Fourier transforms show well-defined peaks corresponding to the round-trip times of periodic orbits in the corresponding classical potential, thereby illustrating the dynamical behavior of the system. Scaled-energy spectroscopy has been applied both to atoms in a magnetic [7,8] and in an electric [9] field. The notion that the positions of Rydberg levels express the classical dynamics of the system also follows from the correspondence principle [10].

Instead of characterizing the system via frequency-resolved measurements, its dynamical behavior can be studied more directly by time-resolved measurements. This can, of course, only be done if the laser pulses are short compared to the orbit times. Since these times are given by the inverse of the dominant frequency spacing of the Rydberg levels, the laser has to have a bandwidth which is larger than that frequency spacing. As a result, several (nondegenerate) eigenstates of the system are excited coherently, i.e., a wave packet is created. The resulting time-dependent wave function is localized in some classical coordinate and will evolve along a classical trajectory in that coordinate. For bound states the wave function is (nearly) periodic and its period matches the orbit time of a classical particle in the potential well. In order to probe this time evolution one can, for example, use a second short laser pulse. Using such a time-resolved method, ten Wolde *et al.* [11] studied the behavior of electronic wave packets in atoms subjected to relatively weak electric fields. The field strength was well below the field needed for field-ionization, resulting in the creation of a (classically) bound wave packet. Another example was given by Yeazell *et al.* [12] who observed wave packet motion along quasi-Landau-orbits in the bound region of the potential in crossed magnetic and electric fields.

Recently, we have reported time-resolved measure-

ments of electronic wave packets that are created in Rb atoms in an electric field, at energies above the classical field-ionization threshold [13]. In a classical picture, field-ionization corresponds to the escape of an electron over the saddle point in the potential of an atom in an electric field. From this potential, $V = -1/r + Fz$, the threshold energy at the saddle point (E_c) is found: $E_c = -2\sqrt{F}$ (atomic units are used unless stated otherwise; F denotes the strength of the electric field that is directed along the z axis). For energies above E_c, the electron in Rb is classically free and its orbits will not be closed, in contrast to bound states. It was, however, found that the orbits can be nearly closed, that is, the electron can return to the region close to the point where it started from, before it escapes from the atom.

In this paper, we present measurements that illustrate the dependence of the dynamics on the polarization of the light. Furthermore, we extend the discussion given earlier [13], which concentrated on the observed orbit times as derived from the peak spacings in the time spectra, to the relative heights of those peaks. Emphasis is put on the connection with the above-mentioned classical picture of field-ionization. In addition, it will be shown that the hydrogenic Hamiltonian accounts for both the dominant orbit times and their scaling with electric field strength.

II. TIME DOMAIN VERSUS FREQUENCY DOMAIN

One may wonder whether it is any use at all to do measurements in the time domain, since all information can already be obtained from the frequency domain. And indeed, the fundamental information content is the same for both domains. However, each type favors a different view on the system under study. The time domain, for example, brings out features related to classical motion. An experimental illustration of this can be found in Ref. [13], where a wave packet performing two simultaneous quantum beats is observed, both corresponding to oscillatory motion in a classical coordinate. The two (different) time periods are immediately clear from the time resolved data but are much less evident from the photoabsorption spectrum (measured by Freeman *et al.* [14]; see Ref. [5] for spectra of other atoms).

Not only for the positions of the energy levels, but also for the lifetimes of the states, each domain has specific situations in which it may be preferred. Insight can be gained with the help of an analogy between a potential (e.g., atomic) and a cavity (e.g., optical) [15]. Characterization of the potential and cavity is done in terms of eigenstates and eigenmodes, respectively. In the case of eigenstates with very long lifetimes (e.g., classically bound states), the corresponding cavity has a very high quality. A frequency scan of the transmission of this cavity (length L) results in sharp resonances, spaced by the free spectral range [$c/(2L)$, with c the speed of light]. The "lifetimes" of the modes can be deduced from the width of a resonance. To obtain the same parameters from a time-resolved measurement, one sends in a pulse which is short compared to the round trip time in the cavity ($2L/c$), and records what comes out as a function of time. This will be a long sequence of pulses, spaced by $2L/c$, with a very slowly diminishing height, implying that it takes a very long time before all information about the system is collected. From these considerations we conclude that long-lived states are more naturally studied in the frequency domain. Note that "long" refers to a time scale which is relative to the round-trip time of the cavity or potential.

In the case of very short-lived (e.g., classically free) states, however, the corresponding cavity has an extremely low quality. The "resonances" in a frequency scan of the transmission can be so broad that they largely overlap, resulting in a frequency spectrum that consists of a small modulation on a large background. It is therefore harder to determine positions and "lifetimes" of the modes than it is for a good-quality cavity. In the time domain, on the other hand, this becomes easier. The transmission of a pulse as a function of time is now given by a small number of pulses, with rapidly decreasing heights, from which the lifetime is immediately apparent. This indicates that short-lived states are more naturally studied in the time domain. Since the frequency and time response are related by Fourier transformation, the background in the frequency spectrum transforms to the instantaneous response in the time spectrum. Furthermore, the relative modulation depth in the frequency spectrum is approximately equal to the inverse ratio of the heights of the instantaneous peak and the next one following in the time spectrum.

The Stark states of Rb above the classical field-ionization threshold, of which we performed a time-resolved study, form an example of such short-lived states. Frequency-resolved measurements of these states can be found in Ref. [14].

III. EXPERIMENTAL PRINCIPLE

Here we will only outline some essential points of the experimental setup, because it is described in detail elsewhere [16]. Instead, we will put emphasis on the quantity obtained in the experiment, namely the time-autocorrelation function of the wave packet.

Short (2.5 ps) laser pulses at a wavelength around 297 nm are sent into a Michelson-interferometer-like arrangement resulting in a pair of identical pulses of which one can be delayed with respect to the other. The key element is a wiggling glass plate in one of the arms of the Michelson, which causes the relative phase between the two pulses to change at a nearly constant rate of $d\phi/dt \approx 2\pi \times 6$ kHz, which is small compared to the repetition rate of the laser (3.8 MHz). In front of the vacuum chamber, which contains the oven with rubibium, the polarization of the light is set with a Soleil-Babinet compensator.

The excitation of ground state ($5s$) Rb atoms by the pulse pair can be described in the following way (see also Ref. [13], and Ref. [17], where the effect of the two-pulse excitation process is linked to Ramsey interference fringes). The first pulse, at time $t = 0$, creates a super-

position of eigenstates $|\psi(0)\rangle$, of which the precise form depends on the transition dipole moments and the electric field of the laser pulse. This superposition evolves to $|\psi(\tau)\rangle$ at time τ, the time of arrival of the second pulse. This pulse also creates a wave packet, which is, neglecting depletion of the ground state, identical to the initial one $|\psi(0)\rangle$, so the total wave function after the pulse sequence is $|\psi_{\rm tot}\rangle = |\psi(\tau) + \psi(0)\rangle$. If the total population in the excited states after one single pulse is written as $P_1 \equiv p\langle\psi(\tau)|\psi(\tau)\rangle = p\langle\psi(0)|\psi(0)\rangle$ (with p a proportionality constant), the resulting total population after two pulses ($P_{\rm tot} = p\langle\psi_{\rm tot}|\psi_{\rm tot}\rangle$) is directly found to be

$$P_{\rm tot} = 2[P_1 + p|\langle\psi(0)|\psi(\tau)\rangle|\cos\chi(\tau)]. \quad (1)$$

Here $\chi(\tau)$ denotes the argument of $\langle\psi(0)|\psi(\tau)\rangle$, the phase difference between the wave packets excited by first and second pulse. Apart from an additional constant, this phase difference is equal to the phase difference between the light pulses, which changes linearly in time due to the wiggling glass plate. Consequently, the total population $P_{\rm tot}$ has a sinusiodal time dependence around the time-independent average value $2P_1$, and the amplitude of the modulation is proportional to $|\langle\psi(0)|\psi(\tau)\rangle|$, the absolute value of the time-autocorrelation function. Since $|\psi(0)\rangle$ results from immediate excitation from the $5s$ ground state of rubidium, it will be confined in the radial direction (due to overlap considerations). Consequently, $|\langle\psi(0)|\psi(\tau)\rangle|$ will be large when $|\psi(\tau)\rangle$ has evolved in such a way that it is again radially confined, which is after one "radial orbit." Furthermore, the angular momentum of $|\psi(0)\rangle$ has mainly p character after excitation with a sufficiently short pulse (due to the $\Delta l = \pm 1$ selection rule). Since l is not a good quantum number in an electric field, angular momentum is not conserved. Therefore, $|\langle\psi(0)|\psi(\tau)\rangle|$ will be large when $|\psi(\tau)\rangle$ again has predominant p character, which is after one oscillation of the angular momentum.

In the experiment, the absolute value of the time-autocorrelation function is obtained directly by calculating the root mean square (RMS) of the final-population signal after passage of this signal through a bandpass filter that isolates the modulated (6 kHz) term. Normalization can be done at $\tau = 0$: $|\langle\psi(0)|\psi(\tau = 0)\rangle| \equiv 1$. Since the atoms were excited above the field-ionization threshold, the "final population" was easily measured by waiting until the atoms ionized and detecting the resulting ions on a multichannel plate (MCP) detector. This was possible because the lifetimes were much shorter than both the time the atoms spent in the interaction region (≈ 1 μs) and the repetition time of the laser (260 ns).

Instead of modulating the relative phase of the pulses, one can also lock the phase. This method has been applied succesfully to, for example, time-resolved measurements of vibrational wave packets in molecules [18] and electronic wave packets in atoms [19], and to coherent control of terahertz radiation in coupled quantum wells [20].

IV. RESULTS AND DISCUSSION

Measurements of the amplitude of the modulation in the final excited-state population have been performed at electric field strengths ranging from 98 to 2745 V/cm. At every field strength the excitation energy E was varied from the zero-field ionization limit $E_0 \equiv 0$ down to considerably below the field-ionization threshold E_c. In addition, the polarization of the laser beam, which progagated perpendicular to the electric field, was taken either parallel or perpendicular to the electric field, or circular. It was found that the dependence of the resulting delay scans on energy and polarization was similar for all field strengths. In Sec. IV C we will show that this is in agreement with the general scaling properties of the Hamiltonian for an atom in an electric field. In the following subsection, results will therefore be shown for only two electric field strengths.

A. General dependence on energy and polarization

In Figs. 1 and 2 results at various excitation energies are given for electric field strengths $F = 1569$ and 196 V/cm, respectively. In all cases, the vertical scale

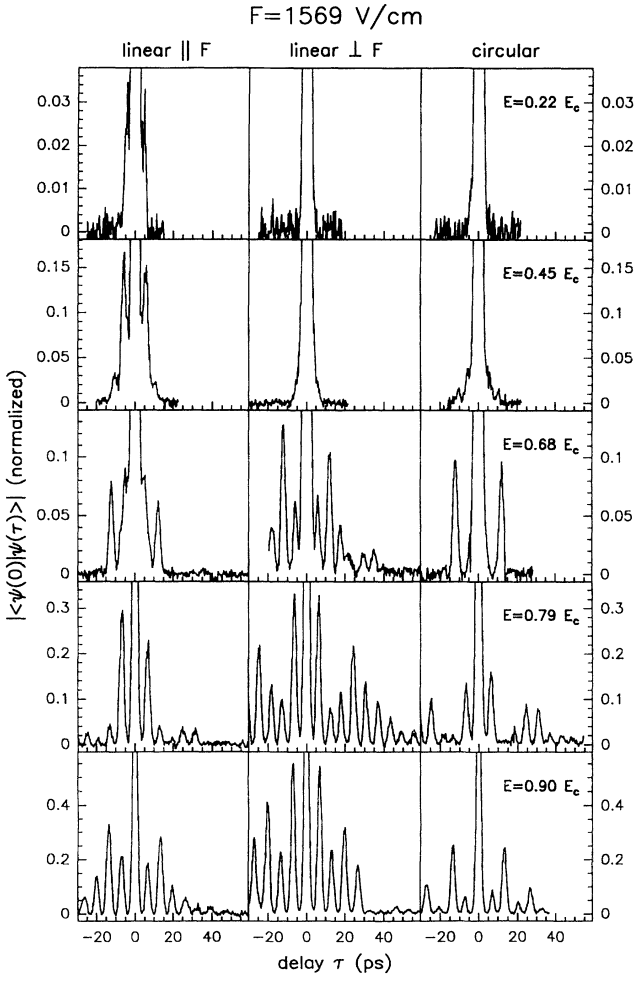

FIG. 1. Results of delay scans measured at an electric field strength of $F = 1569$ V/cm, for three different light polarizations (see text). The excitation energy given in the right column applies to all three scans on the same row ($E_c = -243$ cm^{-1}). Vertical scales are normalized to the peak height at zero delay.

is normalized to the peak height at $\tau = 0$. Note that peaks with a relative height of only $\approx 1\%$ can clearly be resolved. The measuring time at every delay step was ≈ 1.5 s. The energies listed in the figures are normalized to the threshold energy E_c (-243 and -86 cm^{-1}, respectively). The observed trends are discussed in the following paragraphs.

Firstly, less and less structure is seen if the excitation energy is increased. This implies that the lifetimes of the Stark states decrease with increasing energy. Classically it means that fewer and fewer trajectories come back in the vicinity of the core of the atom, the starting point of the trajectory. This is not surprising since the more energy an electron has, the larger the region near the saddlepoint over which it can escape.

The second trend makes this classical picture even more apparent: at energies close to the zero-field limit, the scan with the parallel polarization shows more peaks than the one with perpendicular polarization, while at energies just above the field-ionization limit, the opposite is the case. Excitation with the polarization parallel to the electric field corresponds to classical trajectories

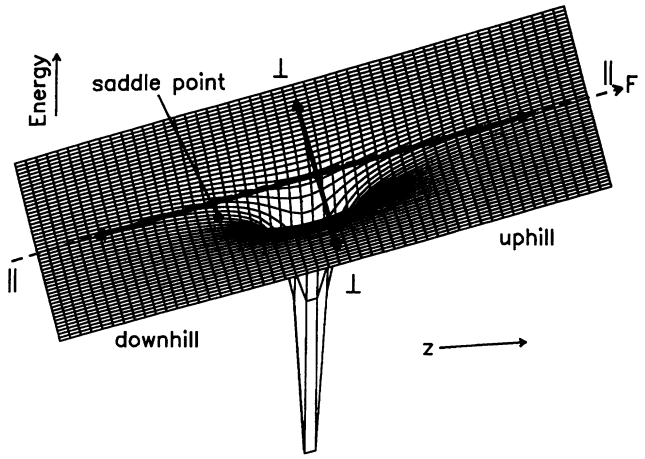

FIG. 3. Potential energy of a combined Coulomb and electric field ($V = -1/r + Fz$). In a classical picture, field-ionization corresponds to the escape of an electron over the saddle point. Light polarizations parallel and perpendicular to the electric field F correspond to trajectories predominantly starting out in the directions marked with ∥ and ⊥, respectively.

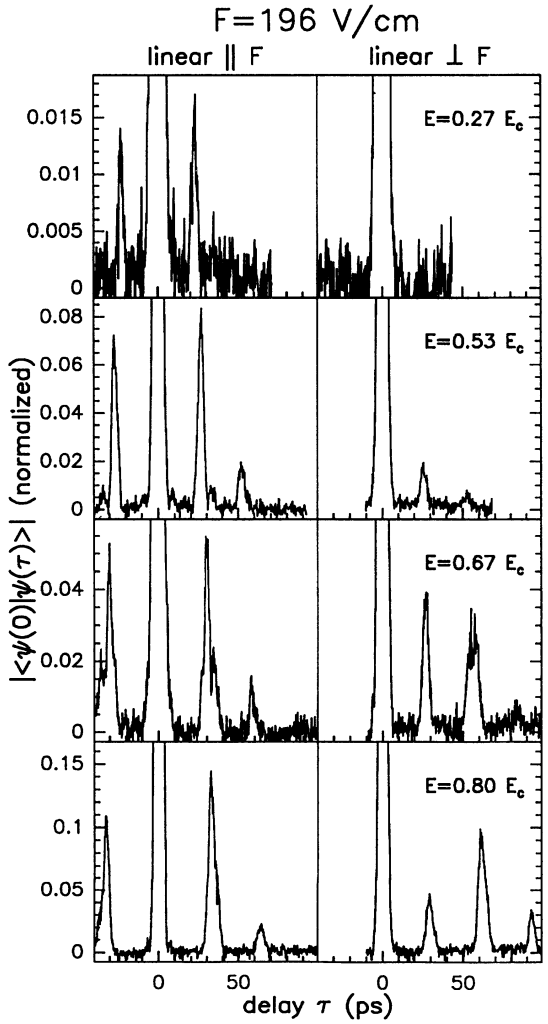

FIG. 2. As Fig. 1, but for $F = 196$ V/cm ($E_c = -86$ cm^{-1}) and only the linear light polarizations.

that predominantly start out in the directions along the electric field (z axis; see Fig. 3). The electrons following trajectories pointing in the direction of the saddlepoint ($-z$ direction) will immediately escape, even for energies just above E_c. On the other hand, the trajectories starting out in the direction pointing away from the saddlepoint ($+z$ direction) travel "uphill," and will always turn around. Therefore they have a good chance of returning to the core region at least once, even at high energies. However, for increasing energy the initial direction needs to be more and more exactly along the z axis, so the contribution from these "uphill" paths still decreases when the energy is raised.

In the case of perpendicular polarization, the initial direction of the trajectories is perpendicular to the field, that is, in the plane $z = 0$ (see Fig. 3). These paths obviously do not come by the saddle point directly. For energies just above E_c, the electron cannot go far out from the origin, so it is almost as if it moves in the $-1/r$ potential in the $z = 0$ plane. As a consequence, the motion almost resembles bound motion, and therefore a large number of recurrences in the delay scans is expected, and definitely more than for parallel polarization, in which case the motion is completely unbound in the direction of the saddle point. At higher energies, however, the electron will go out far from the core in the $z = 0$ plane. Its path is then heavily affected by the sloping plane of the electric field part of the potential, and it will be bent towards the $-z$ direction, which leads to escape of the electron from the atom. So at energies close to E_0, one expects no returns, i.e., no structure, in the perpendicular case, and certainly less than for parallel polarization, where the trajectory starting exactly in the $+z$ direction will always return to the core once.

An instructive bridge between the polarization of the light (E_L) and the starting point of a classical trajectory

is formed by the matrix elements for excitation of Stark states from the ground state. The well known eigenstates of hydrogen in an electric field are labeled $|n\ k\ m_l\rangle$, where $k = -n+1, -n+3, ..., n-1$ is the parabolic quantum number which is related to the conserved dipole moment that is formed by the nucleus and the electron [21]. For $k \approx k_{\max} = n-1$ and $k \approx k_{\min} = -n+1$, the electron density is peaked along the $+z$ ("uphill" part of the potential) and $-z$ ("downhill") direction, respectively. For $k \approx 0$ it is approximately symmetric in the $z = 0$ plane and slightly elongated in the direction perpendicular to the z axis (calculated electron density plots for different k states can be found in Ref. [4]). In first order perturbation theory, the energy of the states is given by

$$E = E_0 - 1/(2n^2) + \tfrac{3}{2}\, nkF, \qquad (2)$$

which shows that the energy of $k > 0$ states is lifted in the field ("blue" Stark states), in accordance with the notion that the electron density is localized "uphill." For excitation from the ground state ($m_l = 0$) with light polarized parallel and perpendicular to the field, the selection rules $\Delta m_l = 0$ and $\Delta m_l = \pm 1$ hold, respectively. The matrix elements to $|n\ k\ 0\rangle$ states are highly peaked for $|k| \approx k_{\max}$, and almost zero for $|k| \approx 0$, while those to $|n\ k\ 1\rangle$ are maximum at $k = 0$ and monotonically decreasing for increasing $|k|$ (for plots of these matrix elements versus k, see, for example, Ref. [2]). Consequently, $\Delta m_l = 0$ ($E_L \parallel F$) implies excitation of states that are peaked along the z axis, and $\Delta m_l = \pm 1$ ($E_L \perp F$) excitation of states that are more or less elongated in the direction perpendicular to the z axis. Although in Rb, m_j, rather than m_l, is a good quantum number, it is more illustrative to describe the creation of a wave packet in terms of the orbital angular momentum m_l, and its corresponding selection rules. This is similar to the notion that a wave packet is said to be created with $l \approx 1$, despite the fact that l is not a good quantum number (see Sec. III). The resonant excitation of an eigenstate is, of course, more logically described with the correct quantum numbers.

In terms of lifetimes of Stark states, the measurements show that $m_l = 0$ states live considerably longer than $|m_l| = 1$ states at energies close to E_0. This can be understood since m_l measures the orbital angular momentum about the z axis, and trajectories starting "uphill" ($+z$ direction) will come back much closer to the core if they have no such angular momentum, because only in that case is their motion constrained along the z axis. Calculations elucidating this point for energies right above E_0 can be found in Ref. [14].

The third observation concerns the structure resulting from excitation with circularly polarized light: roughly speaking, it behaves as an average of the results for parallel and perpendicular polarization. This is not surprising since a mixture of $m_l = 0$ and $|m_l| = 1$ states is excited with circular polarization, classically corresponding to trajectories that start out without a strongly preferred direction.

The fourth trend is the decrease of the peak spacings, that is, the recurrence times, with increasing energy. This relation is shown in Fig. 4 for two different field strengths. The dependence on energy is approximately linear and we will come back to this in Sec. IV F. Here we only note that there was no systematic dependence of the orbit time on light polarization, which is to be expected since, in hydrogenic approximation, the positions of the energy levels are only slightly m-dependent. In first order perturbation theory (linear Stark effect), they are even m-independent. The m-dependence of the *spacing* between the levels of a manifold only shows up in the third and higher order terms [21].

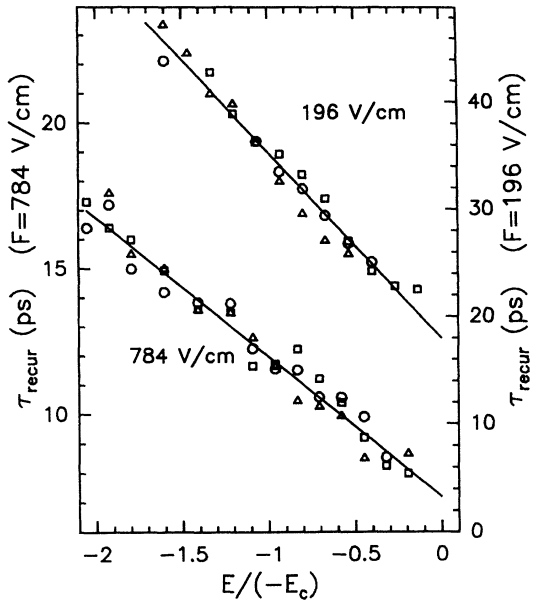

FIG. 4. Measured orbit times as a function of excitation energy relative to the threshold energy for two different field strengths (F = 196 and 784 V/cm, corresponding to $E_c = -86$ and -172 cm^{-1}, respectively). Light polarizations are parallel (squares) or perpendicular (triangles) to the electric field, or circular (circles). The drawn (straight) lines are a guide to the eye.

B. Measurements below the field-ionization limit

When the frequency of the laser was scanned down below the field-ionization limit, a sharp drop in the total ion count rate derived from the MCP detector was observed. The width of the threshold was in agreement with the bandwidth of the laser. However, an almost constant rate was reached at a level of $\lesssim 4\%$ of the count rate above threshold, and this tail disappeared only very slowly as the energy was scanned down further. Typically, it was still $\approx 1\%$ at $E = 2E_C$. We have not been able to determine the ionizing mechanism unambiguously. Electric-field inhomogeneities are improbable because the signal showed no dependence on the precise alignment of the light beam. The cross sections for photoionization of Rydberg states (with ultraviolet light) seem far too small to make ionization by consecutive laser pulses a likely mechanism. It may be that the lifetimes of

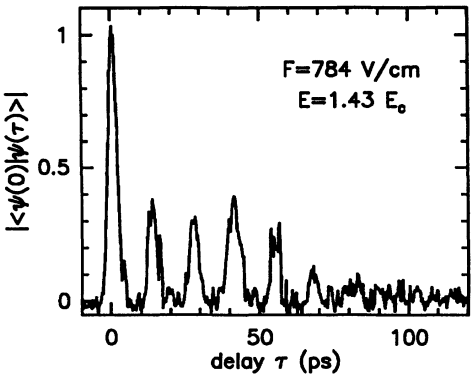

FIG. 5. Example of a result below the field-ionization threshold E_c. Light polarization was perpendicular to the electric field.

some of the Stark states, particularly the "reddest" ones, are sufficiently short to account for part of the the observed signal, but some ionization is also expected to be caused by black-body radiation [22], and collisions with neutral atoms in the interaction region.

Although the signal-to-noise ratio was, of course, much worse in the region below E_c, it was still possible to determine the peak spacings (for an example, see Fig. 5). These were therefore also included in the plots of orbit times versus energy (Fig. 4) as long as they belonged to the regime of strong mixing of the Stark manifolds. Note that no abrupt change in $\tau(E)$ takes place at the field-ionization limit.

C. Scaling of the Hamiltonian

The observation that the signal dependence on energy and polarization is similar for all electric field strengths follows from the scaling properties of the classical Hamiltonian for the hydrogen atom in an electric field:

$$H(p,r,F) = \frac{p^2}{2} - \frac{1}{r} + Fz. \tag{3}$$

Introducing scaled variables $\tilde{p} = pF^{-1/4}$, $\tilde{r} = rF^{1/2}$, and $\tilde{F} = 1$, makes the scaled Hamiltonian field-independent:

$$\tilde{H}(\tilde{p},\tilde{r},1) = \frac{\tilde{p}^2}{2} - \frac{1}{\tilde{r}} + \tilde{z}. \tag{4}$$

From $\tilde{H} = HF^{-1/2}$ it follows that the energy scales as $\tilde{E} = EF^{-1/2}$. Note that $\tilde{E}_c = E_cF^{-1/2} = -2$. In terms of these scaled variables the dynamics of the system are independent of the field strength. The scaling of time (t) follows from the scaling of distance (r) and momentum (p). One finds $t = m\ (r/p) = (m\ (\tilde{r}/\tilde{p}))F^{-3/4} = \tilde{t}F^{-3/4}$ (independent of mass m).

D. Dependence of orbit times on field strength

As a consequence of the scaling of the quantity time with field, one also expects the recurrence times at fixed scaled energy to scale with field according to $\tau \propto F^{-3/4}$. This field dependence was checked for two characteristic values of scaled energy: the zero-field ionization threshold ($\tilde{E}_0 = 0$) and the field-ionization threshold ($\tilde{E}_c = -2$). The corresponding orbit times (τ_0 and τ_c) were derived from the dependence of τ on energy (Fig. 4). Unlike the value for τ_c, which could actually be measured, the value for τ_0 could only be obtained by extrapolation (see Fig. 4). The reason was that no clear peaks were observed for energies very close to E_0 ($E \gtrsim 0.1E_c$), not even for parallel polarization. This extrapolation procedure gave values for τ_0 that are $\approx 20\%$ smaller than the ones we reported in Ref. [13], where τ_0 was taken to be the value actually observed closest to E_0. The values for τ_c are identical to the ones in Ref. [13]. For the field-independent ratio τ_0/τ_c we find 0.53.

The scaling with electric field for both τ_0 and τ_c is given in Fig. 6. The drawn lines correspond to an $F^{-3/4}$ dependence and confirm the expected scaling. Another check on the scaling properties, although not an independent one, is formed by the derivatives $d\tau/dE$ as obtained from Fig. 4 They should scale like $d\tau/dE = (d\tilde{\tau}/d\tilde{E})\ F^{-5/4}$. This is indeed found in Fig. 7.

E. Nature of the orbits

In this section we will discuss what kind of oscillation the observed peaks represent. As mentioned in Sec. I, their spacings correspond to the inverse of the dominant spacing in the frequency domain. In Ref. [13] it was found that this frequency spacing is the spacing between the states within the Stark manifolds, according to Eq. (2) given by $\Delta E_k = 3nF$. If only states within one manifold n_0 are excited, the orbit time of the resulting wave packet is $\tau_k = 2\pi/\Delta E_k = 2\pi/(3n_0F)$. In Ref.

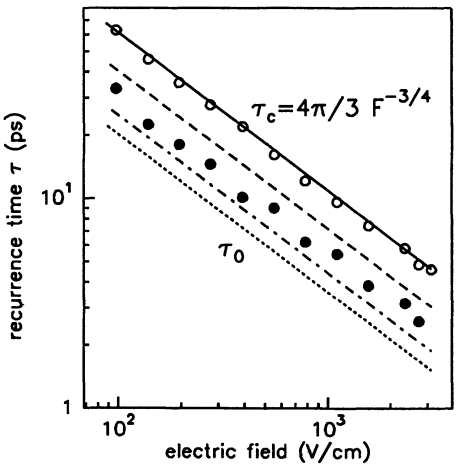

FIG. 6. Observed recurrence times as a function of electric field strength. Open points denote the measured values at the field-ionization limit E_c. The full line is drawn according to Eq. (6). Filled points are the values at the zero-field ionization threshold (E_0) and are obtained by extrapolation (see Fig. 4 and text). The three lower lines, which all have an $F^{-3/4}$ dependence, are given by the following equations: (7) (dashed), (8) (dotted), (9) (dashed-dotted).

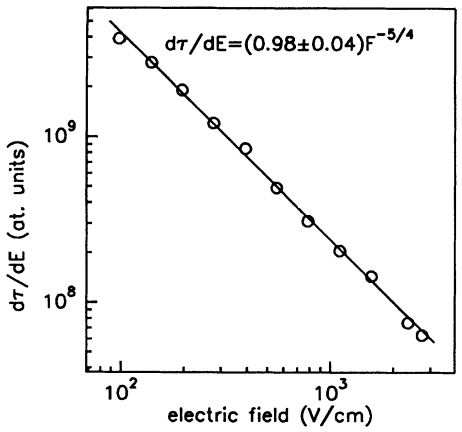

FIG. 7. Derivative of recurrence time versus excitation energy as a function of electric field strength. The derivatives are obtained from measurements as in plots like Fig. 4. The drawn line, of which the equation is given in atomic units, illustrates the $F^{-5/4}$ scaling (see text).

[11] it was shown that this time period corresponds to an oscillation of the magnitude of the angular momentum of the classical orbit between the extreme values $l \approx 0$ and $l \approx n_0 - 1$, that is, a periodic reshaping of the orbit between cigarlike and circular.

Since the present experiment is performed in the regime of strong n mixing, states belonging to many different manifolds are excited. One could, however, still try to use the expression $\tau_k = 2\pi/(3\bar{n}F)$, where $\bar{n}$ now denotes the average n value of all relevant manifolds. Assuming that all spectroscopically accessible $|nk\rangle$ states are essential to the orbit time, a logical $\bar{n}$ is the value of n for which $k = 0$ is excited, so $E = -1/(2\bar{n}^2)$. This results in

$$\tau_k(E,F) = \frac{2\sqrt{2}}{3}\pi\sqrt{-E}F^{-1}. \tag{5}$$

Evaluation at the field-ionization threshold, $E_c = -2\sqrt{F}$, yields

$$\tau_k(E_0,F) = \frac{4\pi}{3}F^{-3/4}. \tag{6}$$

Note that again the $F^{-3/4}$ scaling is found. This Eq. (6), which was also obtained by Rau and Lu [23], represents the full line drawn in Fig. 6. The good fit to the data supports the idea that near E_c indeed all Stark states within the bandwidth of the laser contribute to the return of the wave packet, irrespective of their value of k. Classically, this again implies that at energies near the field-ionization limit almost all trajectories, independent of their starting direction, form nearly closed orbits and do not escape over the saddle point immediately.

In addition to the oscillation in the angular momentum, orbits of another origin can also be observed, namely oscillations in the radial distance to the core. In absence of an electric field, these are formed by making a superposition of states with different principal quantum number n [24]. The orbit time is given by $\tau_n = 2\pi/\Delta E_n = 2\pi n^3$. With the electric field present, they can still be observed provided that the exciting laser pulses are sufficiently short, since close to the field-ionization limit [$F = 1/(16n^4)$] the radial oscillation time τ_n is about five times smaller than τ_k. An experimental example is given in Ref. [13], which shows that the radial oscillations form a modulation on the slower oscillation of the angular momentum.

F. Dependence of orbit times on energy

For fixed electric field, Eq. (5) predicts a square-root dependence of the recurrence time on energy E, $\tau_k \propto E^{1/2}$. This is in contrast to the approximate linear dependence that is observed (see Sec. IV A and Fig. 4). In Fig. 8 expectation and measurement are compared for an arbitrary value of the electric field (this can be done since both follow the same $F^{-3/4}$ dependence). They coincide at the saddle point energy E_c and it is clear that for energies below E_c, Eq. (5) still gives a good description of the observations. In the range of energies $2E_c \lesssim E \leq E_c$, the accuracy of the data simply does not allow discrimination between the $\propto E^{1/2}$ and the linear dependence. We therefore conclude that for energies close to and below the field-ionization threshold, all excited Stark states contribute to the returning part of the wave function.

For energies above E_c, however, Eq. (5) does not describe the observations adequately. The explanation is twofold. Firstly, the assumption under which it was derived, namely that *all* Stark states are essential to the return of the wave packet, is not valid for $E > E_c$. Instead, starting from the reddest one ($k = k_{\min}$), more and more Stark components are lost from the returning part as the energy is increased, as already mentioned in Ref. [13]. This is in agreement with the observation that the lifetimes of the Stark states strongly increase with

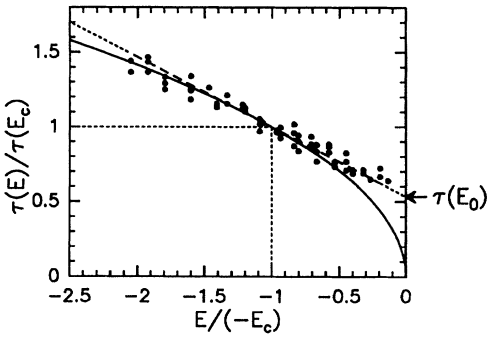

FIG. 8. Full curve represents the $(-E)^{-1/2}$ dependence of the recurrence time on excitation energy, as predicted by Eq. (5). The dashed curve gives the average observed dependence as derived from plots like Fig. 4. The points denote exactly the same data points as in Fig. 4 (so 196 and 784 V/cm and three different light polarizations), but with recurrence time and energy scaled to their respective values at the field-ionization threshold E_c. Equation (5) gives a good description of the data for energies close to and below E_c, but fails for higher energies ($E \gtrsim -0.6|E_c|$).

quantum number k [25]. It is also in accordance with the classical picture of field-ionization, since red Stark states correspond to trajectories starting in the direction of the saddle point and these will be the first not to return as the energy is raised. At even higher energies, the blue components, which start uphill, will also gradually disappear from the returning part of the wave function, until only the bluest one, corresponding to a start in exactly the $+z$ direction, is left over. According to this way of reasoning, one would expect the period of the remaining orbits at E_0 to follow from either the energy spacing of the most blue components within one manifold, $(n,k) = (n_0, n_0 - 1)$ and $(n_0, (n_0 - 1) - 2)$,

$$\tau_k(E_0, F) = 2\pi/\Delta E_k = 2\pi 3^{-3/4} F^{-3/4} = 0.66\ \tau_k(E_c, F), \tag{7}$$

or the spacing between the bluest components of neighbouring manifolds, $(n,k) = (n_0, n_0 - 1)$, and $(n_0+1, (n_0+1) - 1)$:

$$\tau_n(E_0, F) = 2\pi/\Delta E_n = \pi 3^{-3/4} F^{-3/4} = 0.33\ \tau_k(E_c, F). \tag{8}$$

Note that the idea of the gradual loss of Stark components predicts a nonzero orbit time at the zero-field ionization limit, in accordance with the observations, while Eq. (5) predicts a value of zero.

The second reason why Eq. (5) falls short in explaining the orbit times for $E > E_c$ is the fact that perturbation theory, and especially first order, is not very well applicable at energies near E_0. Therefore Rau and Lu used a WKB quantization method to obtain [23]

$$\tau_{\mathrm{WKB}}(E_0, F) = 1.70 F^{-3/4} = 0.41\ \tau_k(E_c, F). \tag{9}$$

Furthermore, Rau argued that this $\propto F^{-3/4}$ scaling with (electric) field is a general property in regimes where two fields of comparable strength are present (strong field-mixing, in this case between Coulomb and electric field) [26]. The result Eq. (9) is more well-known in terms of an energy spacing, $dE/dn = (22.5\ \mathrm{cm}^{-1})/(F/4335\ \mathrm{V/cm})^{3/4}$, and was found to be in agreement with observed resonances around E_0 [6,27,28], which, however, were measured at field strengths typically a few times higher than the ones in our experiment. These resonances have also been explained using a wave packet approach in which outgoing quantum mechanical wave functions are reflected back from the uphill part of the electrical potential and partially go back to the atomic core [29].

All three calculated results for $\tau(E_0, F)$, Eqs. (7), (8) and (9), are given in Fig. 6. The discrepancy between the measurements and the WKB result, which is expected to be correct, is most probably due to the fact that we have not been able to measure $\tau(E_0, F)$ directly, and used an extrapolated value instead (see Sec. IV D).

G. Relative peak heights in one scan

As far as the consecutive peak heights in one delay scan are concerned, the most commonly observed trend is a more or less monotonic decrease with increasing delay. This matches the intuitive picture of a particle in a "nearly closed" classical orbit: after each round trip, it has drifted away from the initial position and impulse coordinates a little further, until it comes so close to the saddle point that it escapes. Note that the peak height thus relates to the stability of the orbit [30]. In terms of the measured quantity $|\langle\psi(0)|\psi(\tau)\rangle|$ one could say that after each oscillation of $|\psi(\tau)\rangle$, it resembles the initial wave function $|\psi(0)\rangle$ a little less.

However, clear deviations from this general trend have been seen. In Fig. 9(a) two recurrences are visible of which the second is about 4.4 times larger than the first. This implies that the orbit is better closed after two round trips than after one. In other words, one could say that apart from the fundamental orbit, there is a much more stable orbit that has twice the fundamental period. Bearing in mind the Fourier relation between the time and frequency domain, some feeling for this apparent "period doubling" can be obtained by considering the positions of the crossing points between the levels of two neighboring Stark manifolds. At electric-field strengths where the levels cross, the dominant frequency spacing is equal to the spacing within one manifold, leading to dominance of the fundamental period in the time domain. At other field strengths, however, the manifolds can be interwoven in such a way that the levels of one manifold lie halfway in between the level of the other. This leads to a dominant frequency spacing which is half the spacing within one manifold, and thus doubling of the period in the time domain.

At lower energies more and more manifolds become important, since more and more red Stark states have lifetimes that are sufficiently long to contribute to the structure in the spectrum. This implies that the number

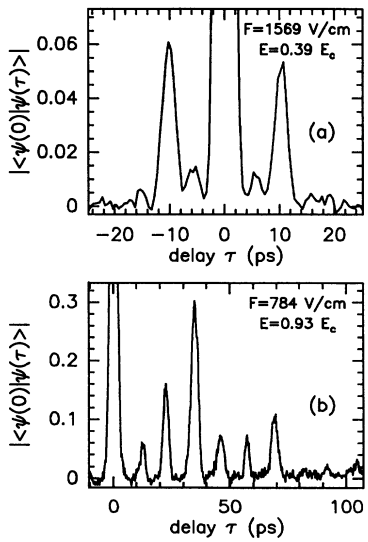

FIG. 9. Two results in which the peaks belonging to the fundamental period are considerably lower than those belonging to a multiple of the fundamental period. (a) Strongest recurrence after twice the fundamental period (light polarization parallel). (b) Strongest recurrence every three times the fundamental period (light polarization perpendicular).

of ways in which the manifolds can intersect grows and, as a consequence, so does the number of possible height distributions. Some examples can be seen in Fig. 1: the result for $E = 0.90E_c$, circular polarization, is another situation where the orbit with the doubled fundamental period is the most stable. In Fig. 9(b) this is even the orbit having a triple period.

Very recently, Gao and Delos have performed semiclassical calculations using closed-orbit-theory for the hydrogen atom in an electric field [31]. They found that the closed orbits of the electron have regular patterns, and that both their number and their possible complexity increase when the energy is lowered from E_0, where only the orbit along the z axis is stable, to E_c. These findings are in accordance with our measurements.

H. Rubidium versus hydrogen

So far we have spoken of classical orbits above the saddle point energy as being "not closed." This is, however, not the case for hydrogen. All blue Stark states are stable in H and the corresponding classical trajectories starting uphill form closed orbits for energies between E_c and E_0. In atoms other than H, k is not a good quantum number. Due to the finite sized ionic core, blue and red Stark states are coupled, so the blue states are no longer stable. In a classical picture the orbit of an electron that starts uphill will, instead of being closed, precess around the core [32], so it will come by the saddle point region sooner or later, thereby leading to ionization. This justifies the picture of unstable orbits in rubidium for energies above the field-ionization threshold.

The coupling between Stark states also affects the positions of the energy levels as compared to hydrogen. In zero field the lowest l states are removed from the "manifold" and in an electric field all level crossings become avoided (for some Stark maps of Rb, see Ref. [5]). One may therefore wonder why a simple hydrogenic formula like Eq. (6) gives such an accurate description of the observed peak spacings at the field-ionization threshold. The reason is twofold. Firstly, the applied electric fields are higher than the fields required for mixing of n-manifolds. Consequently, the low-l states are completely mixed-in in the manifolds again, thereby making the spectrum more hydrogenlike. Secondly, the avoided crossings change the level positions only by small amounts and will therefore only show up in the high-frequency part of the Fourier transform of the frequency spectrum, that is, at relatively long time delays. The positions of the first few peaks, which describe the global level spacings, remain unaffected (see also Ref. [9]). Instead of these rather formal reasons why a hydrogenic approximation gives an adequate description of the observations, one could also argue that this is a general property of highly excited levels, since the electron then spends most of its time far away from the atomic core.

V. CONCLUSIONS

We have presented results of a time-resolved wave packet study of Rb atoms subject to electric fields ranging from 0.1 to 3 kV/cm, at energies close to and above the field-ionization threshold. The observed dependences on excitation energy and light polarization form an illustration of the classical picture of field-ionization, in which an electron escapes over the saddle point in the potential energy. The measured orbit times, as well as their scaling with electric field, are correctly accounted for by the Hamiltonian for hydrogen. This is attributed to the strong mixing of the Stark manifolds and the fact that the first few recurrences in a time-resolved spectrum only contain information on the global, overall structures in a frequency-resolved spectrum, which apparently are not very sensitive to the precise atom at energies above the field-ionization limit.

ACKNOWLEDGMENTS

The authors would like to thank J.H. Hoogenraad for his assistance in the initial stage of this experiment, L.D. Noordam for fruitful conversations and his general support, and W.J. van der Zande for instructive discussions. The work in this paper is part of the research program of the "Stichting voor Fundamenteel Onderzoek van de Materie" (Foundation for Fundamental Research on Matter) and was made possible by financial support from the "Nederlandse Organisatie voor Wetenschappelijk Onderzoek" (Netherlands Organization for the Advancement of Research).

[1] *Rydberg States of Atoms and Molecules*, edited by R.F. Stebbings and F.B. Dunning (Cambridge University Press, Cambridge, 1983).
[2] T.F. Gallagher, *Rydberg Atoms* (in press).
[3] W.R.S. Garton and F.S. Tomkins, Astrophys. J. **158**, 839 (1969).
[4] D. Kleppner, M.G. Littman, and M.L. Zimmerman, in [1].
[5] M.L. Zimmerman, M.G. Littman, M.M. Kash, and D. Kleppner, Phys. Rev. A **20**, 2251 (1979).
[6] R.R. Freeman, N.P. Economou, G.C. Bjorklund, and K.T. Lu, Phys. Rev. Lett. **41**, 1463 (1978).
[7] A. Holle, J. Main, G. Wiebusch, H. Rottke, and K.H. Welge, Phys. Rev. Lett. **61**, 161 (1988).
[8] T. van der Veldt, W. Vassen, and W. Hogervorst (unpublished).
[9] U. Eichmann, K. Richter, D. Wintgen, and W. Sandner, Phys. Rev. Lett. **61**, 2438 (1988).
[10] D.A. Park, *Classical Dynamics and its Quantum Analogues* (Springer-Verlag, Berlin, 1990).
[11] A. ten Wolde, L.D. Noordam, A. Lagendijk, and H.B. van Linden van den Heuvell, Phys. Rev. A **40**, 485 (1989).
[12] J.A. Yeazell, G. Raithel, L. Marmet, H. Held, and H. Walther, Phys. Rev. Lett. **70**, 2884 (1993).

[13] B. Broers, J.F. Christian, J.H. Hoogenraad, W.J. van der Zande, H.B. van Linden van den Heuvell, and L.D. Noordam, Phys. Rev. Lett. **71**, 344 (1993).
[14] R.R. Freeman and N.P. Economou, Phys. Rev. A **20**, 2356 (1979).
[15] L.D. Noordam, B. Broers, A. ten Wolde, H.G. Muller, A. Lagendijk, T.F. Gallagher, and H.B. van Linden van den Heuvell, Physica B **175**, 139 (1991).
[16] J.F. Christian, B. Broers, J.H Hoogenraad, W.J. van der Zande, and L.D. Noordam, Opt. Commun. **103**, 79 (1993).
[17] L.D. Noordam, D.I. Duncan, and T.F. Gallagher, Phys. Rev. A **45**, 4734 (1992).
[18] N.F. Scherer, R.J. Carlson, A. Matro, M. Du, A.J. Ruggiero, V. Romero-Rochin, J.A. Cina, G.R. Fleming, and S.A. Rice, J. Chem. Phys. **95**, 1487 (1991).
[19] R.R. Jones, C.S. Raman, D.W. Schumacher, and P.H. Bucksbaum, Phys. Rev. Lett. **71**, 2575 (1993).
[20] P.C.M. Planken, I. Brener, M.C. Nuss, M.S.C. Luo, and S.L. Chuang, Phys. Rev. B **48**, 4903 (1993).
[21] H.A. Bethe and E.E. Salpeter, *Quantum Mechanics of One- and Two-Electron Atoms* (Plenum Publishing Corporation, New York, 1977).
[22] T.F. Gallagher and W.E. Cooke, Phys. Rev. Lett. **42**, 835 (1979).
[23] A.R.P. Rau and K.T. Lu, Phys. Rev. A **21**, 1057 (1980).
[24] A. ten Wolde, L.D. Noordam, A. Lagendijk, and H.B. van Linden van den Heuvell, Phys. Rev. Lett. **61**, 2099 (1988).
[25] M.G. Littman, M.M. Kash, and D. Kleppner, Phys. Rev. Lett. **41**, 103 (1978); P.M. Koch and D.R. Mariani, *ibid.* **46**, 1275 (1981).
[26] A.R.P. Rau, J. Phys. B **12**, L193 (1979).
[27] W. Sandner, K.A. Safinya, and T.F. Gallagher, Phys. Rev. A **23**, 2448 (1981); H. Rottke and K.H. Welge, *ibid.* **33**, 301 (1986), and references therein; J. Gao, J.B. Delos, and M. Baruch, *ibid.* **46**, 1449 (1992).
[28] W.L. Glab, K. Ng, D. Yao, and M.H. Nayfeh, Phys. Rev. A **31**, 3677 (1985).
[29] W.P. Reinhardt, J. Phys. B **16**, L635 (1983); D. Wintgen, *ibid.* **22**, L5 (1989); G. Alber, Phys. Rev. A **40**, 1321 (1989); J. Gao and J.B. Delos, *ibid.* **46**, 1455 (1992).
[30] D. Wintgen, Phys. Rev. Lett. **58**, 1589 (1987).
[31] J. Gao and J.B. Delos, Phys. Rev. A (to be published).
[32] C. Fabre and S. Haroche, in [1].